International Journal of Advance Interdisciplinary Research
Vol. 01(01), June 2025, pp. 1-09, e-ISSN: 3107-913X
DOI 10.66095/mkses/ijair.2025.v1.i1.1

# Bandgap engineering of the perovskite materials for solar cell applications

[1]R. K. Shukla, [2]Amrit Kumar Mishra and [3]Susheel Kumar Singh
[1]Department of Physics, University of Lucknow, Lucknow - 226007, U.P. (India)
[2]Department of Physics, University of Lucknow, Lucknow - 226007, U.P. (India)
[3]Department of Physics, HLYB P.G. College Lucknow U. P. (India)
E-mail: rajeshkumarshukla_100@yahoo.co.in

## Abstract:

Nowadays, Perovskite materials are frequently used in the application of solar cells. We are using organic-inorganic halide like $CH_3NH_3PbI_3$, $CH_3NH_3PbCl_3$ and $CH_3NH_3PbBr_3$ in which $CH_3NH_3$ is organic part, Pb is the inorganic part and I, Cl, Br is the halide atom. Perovskite solar cells, which are widely employed in energy harvesting materials for applications in solar cell, are one of the types of solar cells that I have worked on recently. From 3.8% in 2009 to 23% in 2020, perovskite solar cells' power conversion efficiency has grown significantly. I became interested in perovskite solar cells because of its high efficiency, long diffusion length, high photon absorption capacity, high mobility, low cost, and simple production procedure. High power conversion efficiencies have been successfully achieved through the investigation of photovoltaic systems in conjunction with tandem sun cells. However, this intriguing idea has not been sufficiently implemented in perovskite solar cells. The viability of employing perovskite semiconductors with varying bandgaps in conjunction with standard crystalline silicon for tandem concentric solar cell applications is evaluated in this paper. We assess the tandem perovskite concentrator solar cells' device performance.

**Keywords:** perovskite, diffusion length, band gap, efficiency.

## 1. Introduction:

Nowadays, perovskite material is frequently used in solar cell devices as an active layer. Using the perovskite (CH3NH3PbI3) photovoltaic material's crystal structure, A stands for the material's organic component (CH3NH3), B for its inorganic component (Pb), and O for the halide atoms (such as Cl, Br, and I). In the perovskite (CH3NH3PbI3), phase transitions take place at 327 K from cubic to tetragonal structure and at 160 K from tetragonal to orthorhombic structure [1]. Figure 1 displays the perovskite materials' ABO3 crystal structure.

International Journal of Advance Interdisciplinary Research
Vol. 01(01), June 2025, pp. 1-09, e-ISSN: 3107-913X
DOI 10.66095/mkses/ijair.2025.v1.i1.1

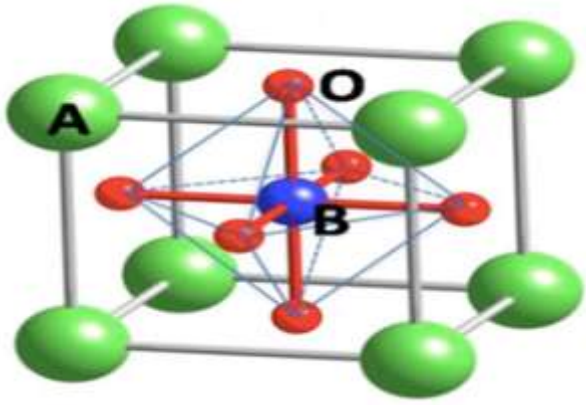


**Figure 1: The crystalline $ABO_3$ structure of the Perovskite materials**

The extraordinary material properties of the perovskite solar cell have a major role for the frequently used perovskite material in the device physics; T perovskite material has low excition binding energy, high absorption coefficient, a long charge carrier diffusion length, and tuneable band gap [2-7]. Although the efficiency of lab-scale devices is higher than commercially existing solar cells, perovskite solar cells have stability issues because they degrade over time due to a variety of factors, including air, light soaking, thermal stress (heat), UV light exposure, electric fields, humidity, and many more [8–10]. Due to this factor, we could not achieve the market requirement. Hence, we focused on the detailed degradation study of the perovskite solar cell for the improvement of device stability. UV filters, device encapsulation, and inhibiting trap states (air and humidity-induced deterioration), UV radiation, and electric fields, respectively, are employed to improve stability [11–14]. During the operation of the perovskite solar cell thermal stress degradation occurs due to this, we will first focus on the structural change of perovskite material with a temperature change of the device. This work focusses on the intrinsic degradation processes of the perovskite absorber layer, which include chemical, optical, and morphological deterioration, among other layers that make up the device.

## 2. Fabrication of Device

The newly developed spin coating process used to fabricate the solar cells is depicted in Figures 2(a), 2(b), 2(c), and 3.

Zn metal powder and diluted HCl are used to etch patterned fluorine-doped tin oxide surfaces (FTO). The etched FTO was cleaned by sequentially sonicating it for 15 minutes in soap solution, deionised water, and isopropanol. $TiO_2$ (hole blocking layer) is then applied to it using the spin coating process, which involves spinning at 5000 rpm for 45 seconds and

International Journal of Advance Interdisciplinary Research
Vol. 01(01), June 2025, pp. 1-09, e-ISSN: 3107-913X
DOI 10.66095/mkses/ijair.2025.v1.i1.1

heating it to 4500 C for 25 minutes. The mixture is made up of 75 microlitres of concentrated HCl, 7.25 millilitres of ethanol, and 0.5 millilitres of Ti (IV) isopropoxide (Sigma Aldrich). use a diluted Dyesol 18 N-RT paste solution (1:3.5 w/w in ethanol) for 30 seconds at 4000 rpm and heating it to 5000C for 30 minutes results in a 360 nm film thickness. This creates a TiO2 mesoporous layer.

**2.1 Perovskite Preparation:**

TiO2 films were made inside the box for the perovskite deposition process. They deposited the perovskite layer.

**2.2 $TiCl_4$ Treatment:**

Initially, we mix 1 milliliter of 2M TiCl4 with 100 milliliters of DI water, place the TiO2 films in the mixture, and then bake the film at 800 degrees Celsius. The film is then cleaned using water, ethanol, and dry Ar gas before being heated for 30 minutes at 5000°C. Next, we spin-coat a 1 M PbI2 (462 mg) solution in 1 ml of DMF for 5 seconds at 6000 rpm. After 25 minutes of heating at 700°C on a hot plate, the PbI2 film is dipped in the aforementioned solution for 15 minutes, dropped into MAI (8 mg/ml) in isopropanol, and then washed.

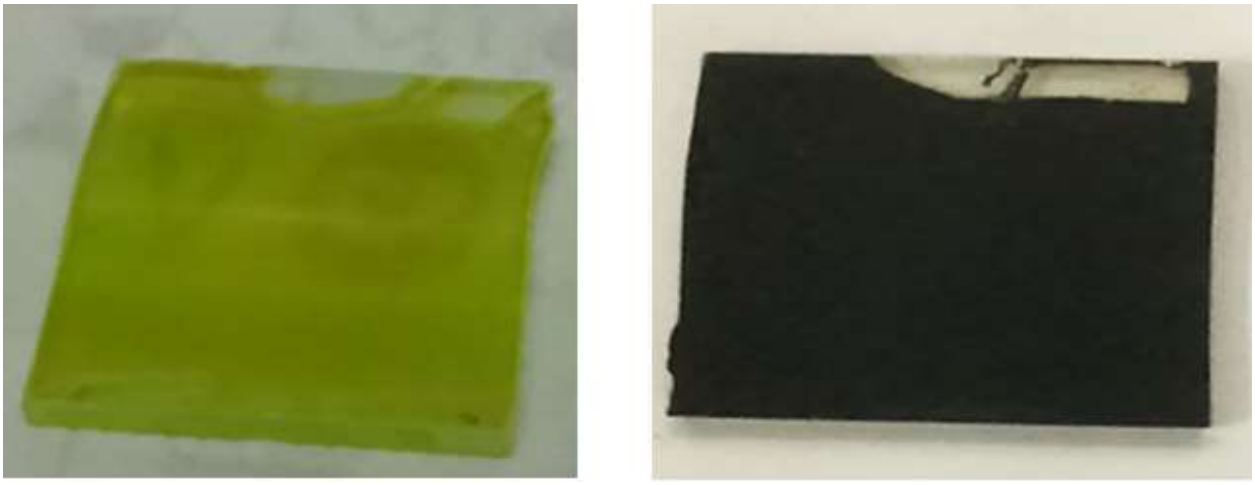

**Figure 2(a): $PbI_2$ layer deposition onthe FTO glass; (b): $CH_3NH_3PbI_3$ layerdeposition on FTO glass.**

International Journal of Advance Interdisciplinary Research
Vol. 01(01), June 2025, pp. 1-09, e-ISSN: 3107-913X
DOI 10.66095/mkses/ijair.2025.v1.i1.1

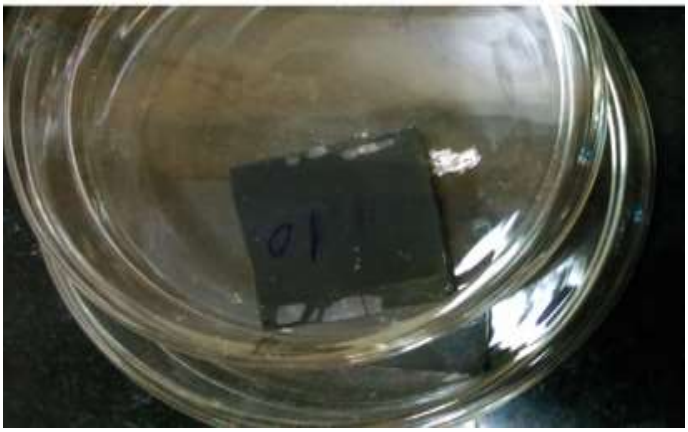

**Figure 2(c): perovskite film in the desiccator**

### 2.3 Spiro-MeOTAD Layer Deposition:

Using a spin coater set to 4000 rpm for 30 seconds, we first mix chlorobenzene (1 mL) with Spiro-MeOTAD (100 mL), TBP (tursary butyl pyridine) (28.5 μL), and Li salt solution (17.5 μL). Then, we use a thermal evaporator to deposit gold onto the Spiro-MeOTAD layer.

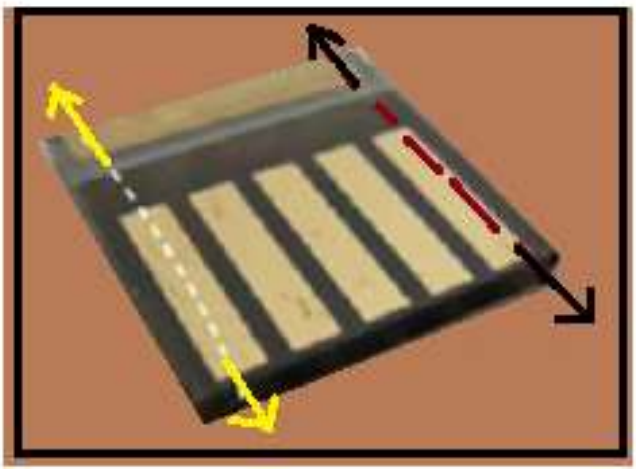

**Figure 3: The perovskite solar cell (the region under the Arrow showed the active area of the device)**

### 3.0 Electrical characterization of the perovskite solar cell:

- J-V Characteristics
- C-V Characteristics
- C-f Characteristics
- I-Rh (%), Current – Relative humidity spectra.
- I-t, Current – Time spectra

- Noise spectroscopy

### 3.1 J-V Characteristics

The perovskite solar cell's J-V measurements were conducted using a Keithley 2450 source-measure unit under the AM1.5G 100 mW/cm2 solar spectrum, and the PM-100 A small power meter was used to measure the light intensity. The device under test (DUT) had an applied voltage between +5 and -5 V, and the scan rate was 200 mV/s.

### 3.2 C-V Characteristics

The apparatus used for the capacitance-voltage measurements of the perovskite solar cell were 4 MHz DSP Lock-in amplifier, Stanford Research System SR 865 A, and key sight 33621 A waveform generator.

### 3.3 C - f Characteristics

The SR 865 A, SR 560 voltage pre-amplifier, 4 MHz DSP Lock-in amplifier, and 33621 A waveform generator were used to test the C-f of the perovskite solar cell.

### 3.4 Current - Relative humidity I-Rh (%), Curve

The electrical current versus relative humidity spectrum was observed in the perovskite solar cell by applied +5 V to -5 V DC source to the DUT (device under test) by Keithley 2450 source - measure unit under the AM1.5G 100 $mW/cm^2$ solar spectrum. Humidity control is done by sending wet nitrogen, dry nitrogen, humid air, or dry airflow to the humidity control chamber.

### 3.5 I-t, Current -Time spectra

The electrical current versus time spectrum was observed at a fixed humidity level in the perovskite solar cell by applied +5 V to -5 V DC source to the DUT (device under test) by Keithley 2450 source - measure unit under the AM1.5G 100 $mW/cm^2$ solar spectrum.

### 3.6 Noise spectroscopy

Analyzing noise can help explain the electrical properties of defect states and charge carrier dynamics, which are important factors in determining the photovoltaic modules s and quality of heterojunction solar cell [4-5]. A useful tool for explaining charge carrier injection, defect states, photovoltaic material mobility, and how the 1/f noise spectrum changes as a result of perovskite solar cell deterioration is the 1/f noise spectrum seen in typical perovskite solar cells. In the low-frequency region, 1/f noise predominates, and its spectral density is proportional to 1/f. The device parameter variation over time is modelled using low-frequency 1/f noise.

International Journal of Advance Interdisciplinary Research
Vol. 01(01), June 2025, pp. 1-09, e-ISSN: 3107-913X
DOI 10.66095/mkses/ijair.2025.v1.i1.1

## 4.0 Structural, Morphological and simulation of the perovskite solar cell

### 4.1 X-Ray diffraction

Understanding the crystal structure of bulk solids, thin films, including the lattice constant, orientation of polycrystalline films, geometry, identification of unknown materials, defects, stress, particle size determination, etc., is made possible by condensed matter physics XRD investigation, which is vital in the field of material science. Neutrons and electrons are also employed in material diffraction investigations.

Mathematically, Bragg's law is bellowed.

$$2d\sin\theta = n\lambda$$

where d is the atoms' interplanar spacing, n is the order of diffraction, λ is the light wavelength employed in the XRD analysis, and θ is the X-ray glancing angle. After that, the pattern may be compared to database cards from the Joint Committee on Power Diffraction Standards (JCPDS) or any other published study. Consequently, Figure 4 provides identification.

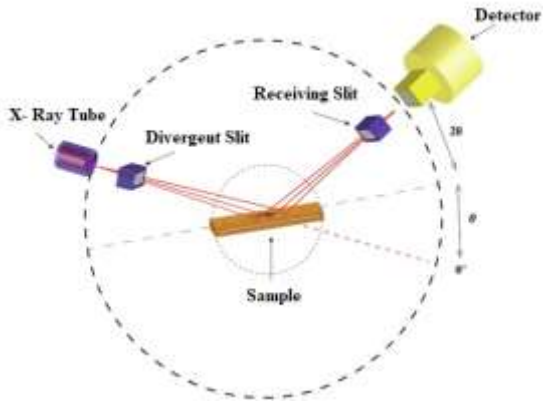


**Figure 4: The schematic diagram of the X-Ray Diffractometer**

### 4.2 Scanning electron microscope (SEM)

In the subject of material science, the use of SEM is investigated to comprehend the sample's surface morphology. The highly advanced electron microscope, SEM scan a sample's surface with the help of using an intense electron beam to in order to create a picture. Atoms and electrons in the sample interact to produce a range of signals that offer information about the surface shape, sample's composition, and other characteristics like electrical conductivity.

International Journal of Advance Interdisciplinary Research
Vol. 01(01), June 2025, pp. 1-09, e-ISSN: 3107-913X
DOI 10.66095/mkses/ijair.2025.v1.i1.1

The scanned electron beam creates a pattern, and a picture is created by combining the beam's position with the strength of the signal it detects.

The thickness of the films may be determined using a SEM of the transverse cross-section of a homogenous sample. Secondary imaging, the most popular or standard detection technique, uses a scanning electron microscope to create a very high-resolution picture of a sample surface that reveals features smaller than 1 nm. A significant depth of field is made possible by the tremendously tapered beam of electron, giving the sample a distinctive 3D appearance that is helpful in determining its surface structure. Figure 10 displays the schematic diagram of the SEM's image generation mechanism.

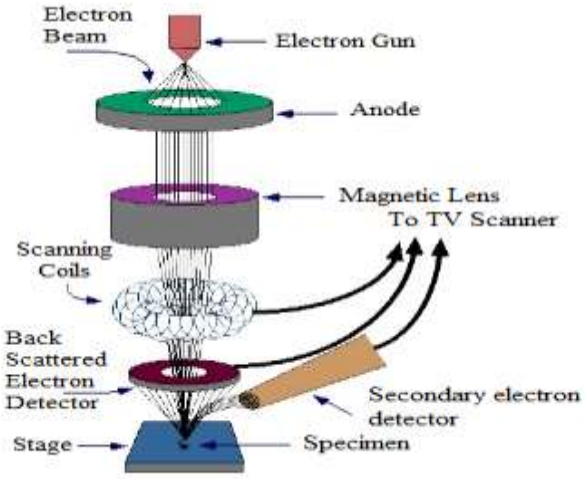


**Figure 10: The diagrammatic representation of the image formation system of SEM**

## Conclusion

In order to explain the chemical and physical properties of the perovskite solar cell, we discussed its history, bandgap engineering, and various experimental characterization techniques. We also discussed the fundamental physics of solar cells and the types of solar cells, as well as why perovskite is a good material for energy harvesting in the field of material science. At the moment, the commercial and private PV markets are dominated by crystalline silicon solar cells. These devices have a high efficiency (>25%). In contrast to thin-film PV technology, these solar cells are heavier, thicker, and more stiff. Certain markets, such extraterrestrial solar panels, have already adopted thin-film photovoltaics. Nevertheless, extremely costly or hazardous chemicals are frequently used in thin-film solar cells with high efficiency (>25%).

## Reference

[1] Tanzila Tasnim Ava, Abdullah Al Mamun, Sylvain Marsillac and Gon Namkoong**.** A Review: Thermal Stability of Methylammonium Lead Halide Based Perovskite Solar Cells. Appl. Sci. **2019**, 9, 188; doi: 10.3390/app9010188.

[2] Hao, F.; Stoumpos, C.C.; Cao, D.H.; Chang, R.P.; Kanatzidis, M.G. Lead-free solid-state organic–inorganic halide perovskite solar cells. Nat. Photonics **2014**, 8, 489. [CrossRef]

[3] Lin, Q.; Armin, A.; Nagiri, R.C.R.; Burn, P.L.; Meredith, P. Electro-optics of perovskite solar cells. Nat. Photonics **2015**, 9, 106. [CrossRef]

[4] Miyata, A.; Mitioglu, A.; Plochocka, P.; Portugall, O.; Wang, J.T.W.; Stranks, S.D.; Snaith, H.J.; Nicholas, R.J. Direct measurement of the exciton binding energy and effective masses for charge carriers in organic-inorganic tri-halide perovskites. Nat. Phys. **2015**, 11, 582–587. [CrossRef]

[5] Stranks, S.D.; Eperon, G.E.; Grancini, G.; Menelaou, C.; Alcocer, M.J.; Leijtens, T.; Herz, L.M.; Petrozza, A.; Snaith, H.J. Electron-hole diffusion lengths exceeding 1 micrometer in an organometal trihalide perovskite absorber. Science **2013**, 342, 341–344. [CrossRef]

[6] Xing, G.; Mathews, N.; Sun, S.; Lim, S.S.; Lam, Y.M.; Grätzel, M.; Mhaisalkar, S.; Sum, T.C. Long-range balanced electron-and hole-transport lengths in organic-inorganic CH3NH3PbI3. Science **2013**, 342, 344–347.[CrossRef]

[7] Noh, J.H.; Im, S.H.; Heo, J.H.; Mandal, T.N.; Seok, S.I. Chemical management for colorful, efficient, and stable inorganic–organic hybrid nanostructured solar cells. Nano Lett. **2013**, 13, 1764–1769. [CrossRef] [PubMed]

[8] Niu, G.; Guo, X.;Wang, L. Review of recent progress in chemical stability of perovskite solar cells. J. Mater. Chem. A **2015**, 3, 8970–8980. [CrossRef]

[9] Grätzel, M. The light and shade of perovskite solar cells. Nat. Mater. **2014**, 13, 838. [CrossRef] [PubMed]

[10] Li, X.; Tschumi, M.; Han, H.; Babkair, S.S.; Alzubaydi, R.A.; Ansari, A.A.; Habib, S.S.; Nazeeruddin, M.K.; Zakeeruddin, S.M.; Grätzel, M. Outdoor performance and stability under elevated temperatures and long-term light soaking of triple-layer mesoporous perovskite photovoltaics. Energy Technol. **2015**, 3, 551–555. [CrossRef]

[11] Han, Y.; Meyer, S.; Dkhissi, Y.; Weber, K.; Pringle, J.M.; Bach, U.; Spiccia, L.; Cheng, Y.B. Degradation observations of encapsulated planar CH3NH3PbI3 perovskite solar cells at high temperatures and humidity. J. Mater. Chem. A **2015**, 3, 8139–8147. [CrossRef]

[12]. Leijtens, T.; Eperon, G.E.; Pathak, S.; Abate, A.; Lee, M.M.; Snaith, H.J. Overcoming ultraviolet light instability of sensitized TiO2 with meso-superstructured organometal tri-halide perovskite solar cells. Nat. Commun.**2013**, 4, 2885. [CrossRef]

[13] Chen, W.; Wu, Y.; Yue, Y.; Liu, J.; Zhang, W.; Yang, X.; Chen, H.; Bi, E.; Ashraful, I.; Grätzel, M.; et al. Efficient and stable large-area perovskite solar cells with inorganic charge extraction layers. Science **2015**, aad1015.

[CrossRef]

[14] Shao, Y.; Yuan, Y.; Huang, J. Correlation of energy disorder and open-circuit voltage in hybrid perovskite solar cells. Nat. Energy **2016**, 1, 15001.